Supplementary material accompanying the manuscript: "Lateral flexure of the Erebus Ice Tongue due to ocean current forcing and fast ice coupling"

Rodrigo Gomez-Fell 1∗ , Wolfgang Rack 1, Heather Purdie 1,2, Oliver J. Marsh 3, Christian Wild 4

1 Gateway Antarctica, School of Earth and Environment, University of Canterbury, Christchurch, New Zealand.

2 School of Earth and Environment, University of Canterbury, Christchurch, New Zealand.

3 British Antarctic Survey, Cambridge, UK.

Supplementary Figures

In the supplementary material, we present some figures referenced in the text. Fig. S1 shows the thickness data from BedMachine V2 (Morlighem M, 2020) and the corrections used; Fig. S2 compares tide gauge data from McMurdo Sound and a tidal model; Fig. S3 is a schematic of the ice tongue and the variable used in the analytical model; Fig. S4 shows the mechanical effective area used in the lateral bending analytical model; Fig. S5 is a scatter plot of the relation between DInSAR displacement in fringes compared to the differential tidal currents from the CATS2008 tidal model when fast ice is absent; and Fig. S6 is a contour plot of the flexure in relation to changes in the drag coefficient (C_d) and the Elastic Modulus (E_b).
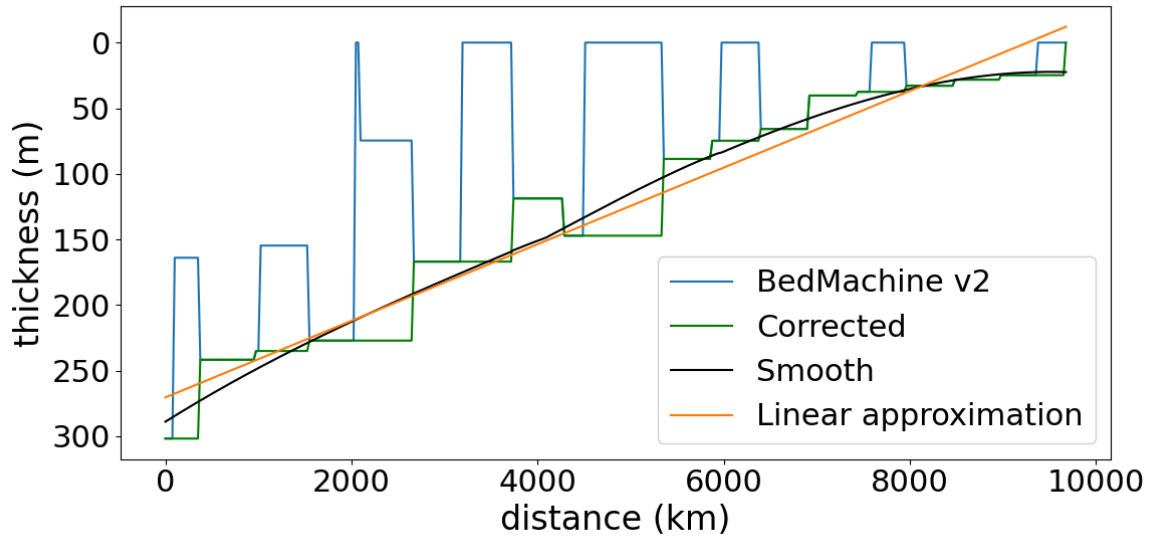
Fig. S1 shows the thickness data from BedMachine at the centre line in blue, the corrected thickness in green, and the smooth thickness in black. In orange is the linear approximation used for deriving the momentum.
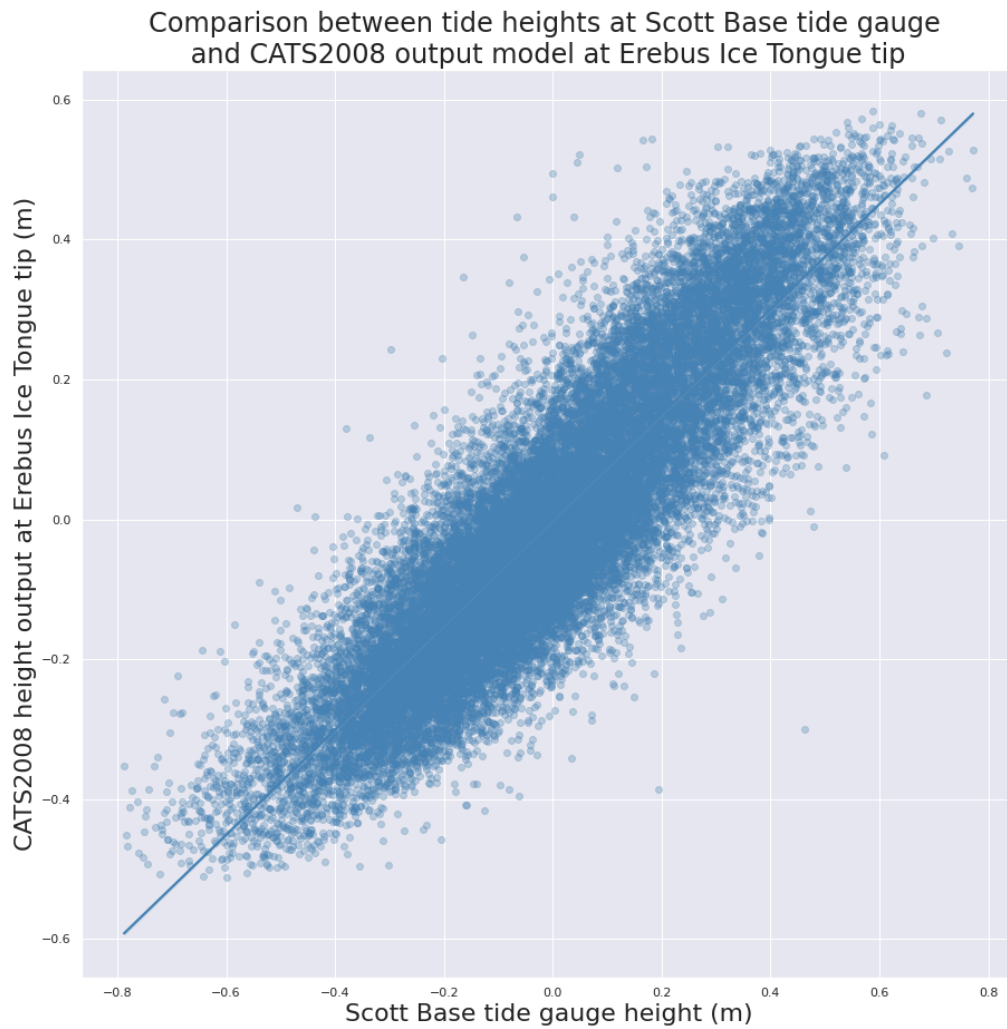
Fig. S2 - Four years (Feb-2016 to Jan-2020) of tidal data from the tidal gauge at McMurdo Sound are compared with the CATS2008 (Padman and others, 2002) model output at the tip of the Erebus Ice Tongue. The two data sets have a significant (p-value<0.05) 0.88 Pearson correlation.
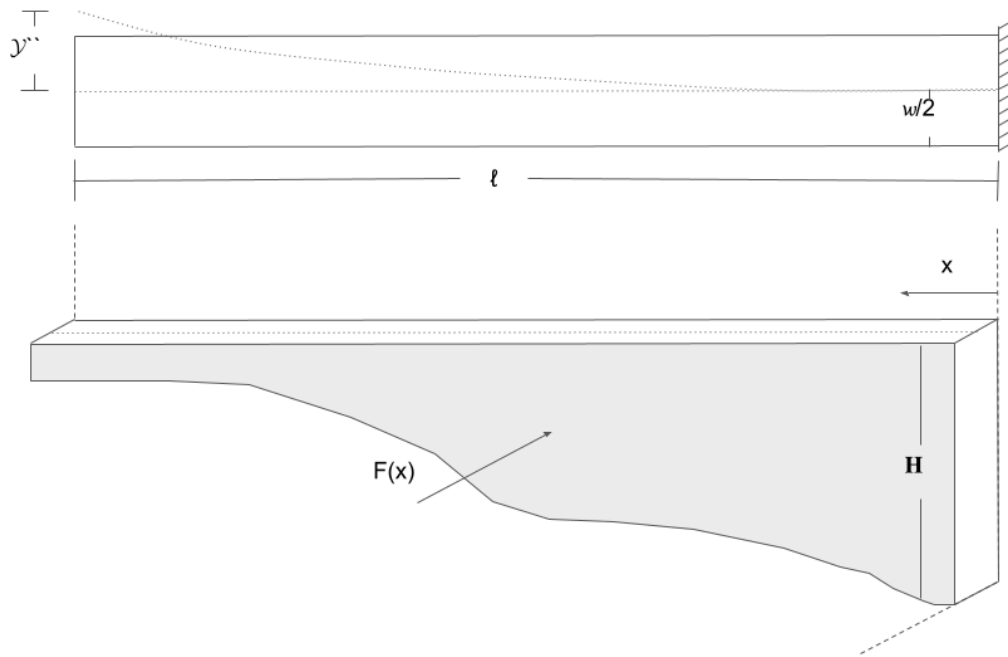
Fig. S3 - Schematic of the Erebus Ice Tongue, showing the variables associated with the analytical model: w width, y' maximum bending, l total ice tongue length, x distance from GL, H thickness and F(x) force applied by currents orthogonal to the ice tongue.
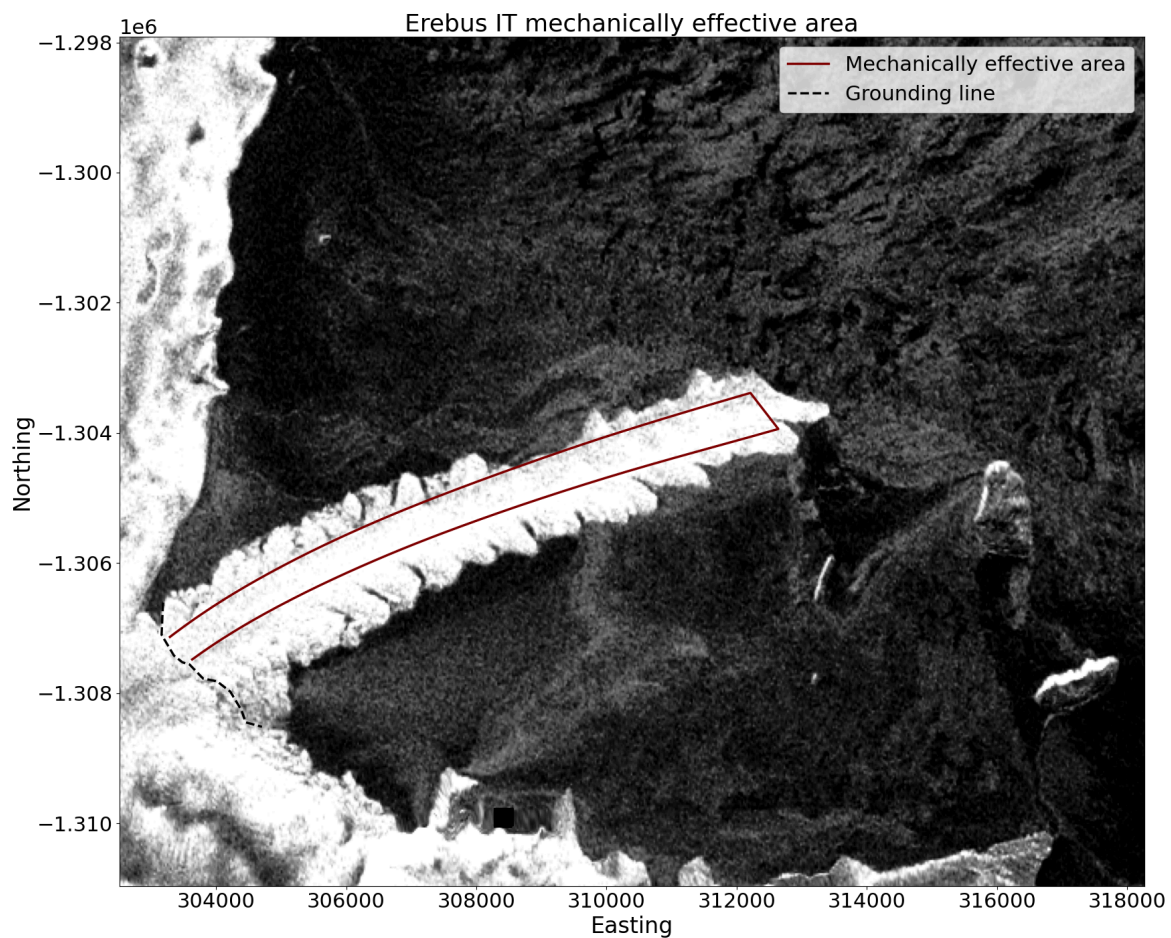
Fig. S4 - The figure shows the flowlines based on ice flow trajectories seeded at the grounding line of the Erebus Ice Tongue (dashed black line). The flowlines encompass the mechanically effective area used for the analytical model, boxed by brown lines and the grounding line. The figure is in WGS 84 / Antarctic Polar Stereographic EPSG:3031.
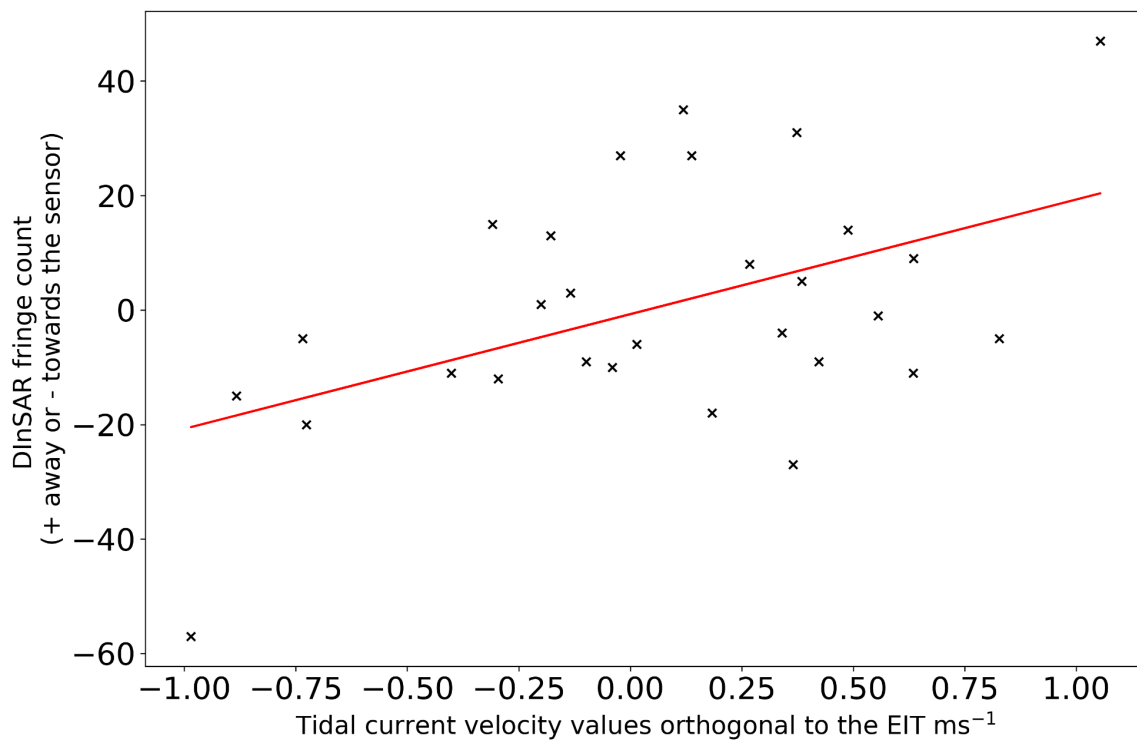
Fig. S5 - Scatter plot of the relation between DInSAR displacement in fringes compared to the differential tidal currents from the CATS2008 tidal model when fast ice is absent. The linear regression in red has an R-squared of 0.23 and a p-value of 0.0079.
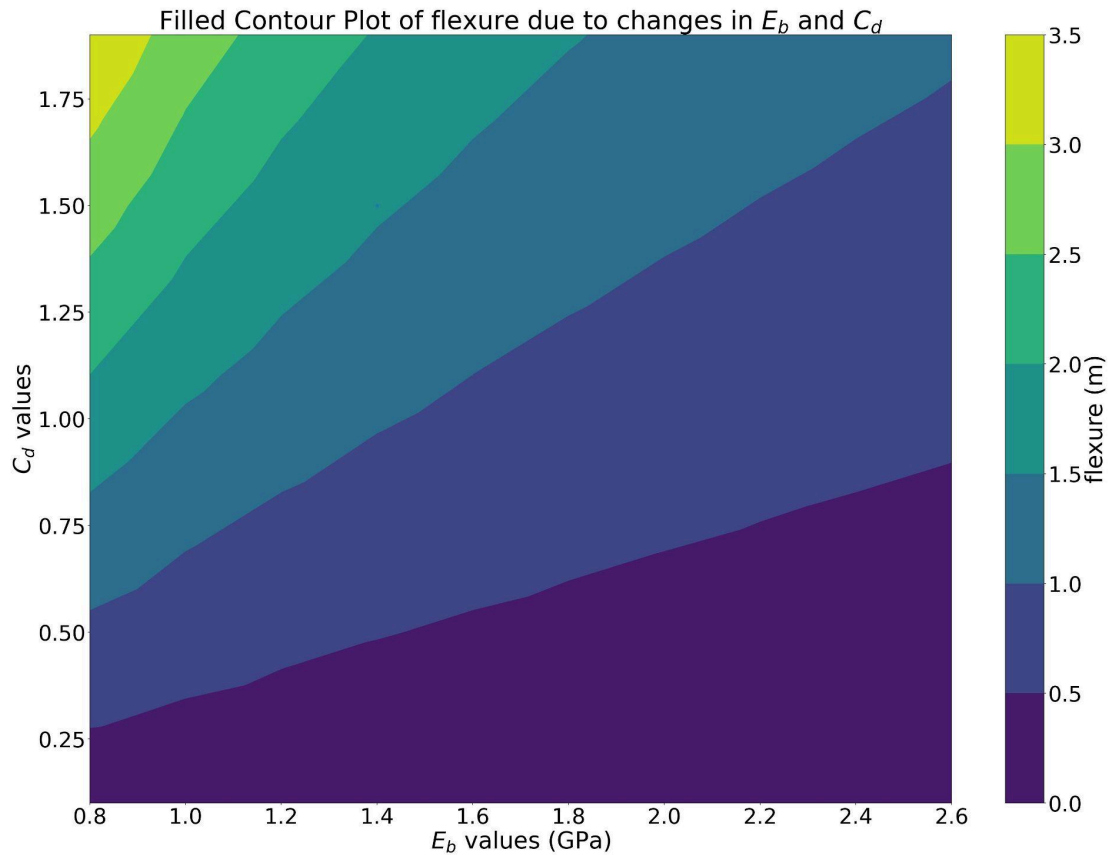
Fig. S6 - Contour plot of the flexure in relation to changes in the drag coefficient (C_d) and the Elastic Modulus (E_b) associated with the geometry and length of the Erebus Ice Tongue at the moment of the study.

Supplementary video

Video S1 - The flexure pattern of the Erebus Ice Tongue associated with each DInSAR image is presented in a video file EIT_bend_2017-2020.gif.

References

Morlighem M (2020) MEaSUREs BedMachine Antarctica [Data set]. (doi:https://doi.org/10.5067/E1QL9HFQ7A8M)

Padman L, Fricker HA, Coleman R, Howard S and Erofeeva L (2002) A new tide model for the Antarctic ice shelves and seas. Annals of Glaciology, 34, 247–254, ISSN 0260-3055 (doi: 10.3189/172756402781817752)